

## New developments in conformal tracking for the CLIC detector

ERICA BRONDOLIN

*On behalf of the CLICdp collaboration,  
Experimental Physics Department at CERN  
Geneva, Switzerland*

### ABSTRACT

Conformal tracking is an innovative track finding strategy adopted for the detector at the Compact Linear Collider (CLIC), a proposed future electron–positron collider. It features a pattern recognition in a conformal-mapped plane using the cellular automaton algorithm to reconstruct the trajectory of charged particles in a magnetic field. The efficiency and robustness of the algorithm are validated using full-simulation studies in the challenging beam-induced background conditions expected for the 3 TeV stage of the CLIC collider. The tracking performance requirements, set by the ambitious CLIC physics programme, have been shown to be met. Moreover, thanks to its flexibility and geometry-agnostic nature, this algorithm was also shown to be easily adaptable to different detector designs and beam conditions.

### PRESENTED AT

Connecting the Dots and Workshop on Intelligent Trackers (CTD/WIT 2019)  
Instituto de Física Corpuscular (IFIC), Valencia, Spain  
April 2-5, 2019

## 1 Introduction

The next generation of tracking detectors foreseen for future electron–positron colliders, such as the Compact Linear Collider (CLIC), will feature ultra-low-mass systems and provide extremely high position accuracy to fulfil the requirements imposed by the physics programme and the challenging beam-induced background conditions. In order to fully exploit these features in track reconstruction, a new track finding technique was developed by the CLICdp collaboration that merges the two concepts of conformal mapping and cellular automaton. We refer to this technique as *conformal tracking*. Thanks to its flexibility and robustness, the new algorithm can also be adapted easily to different detector designs and geometries.

The goal of this paper is to describe the conformal tracking algorithm, its implementation as well as its performance in the track reconstruction used in the CLIC detector (CLICdet). Section 2 introduces the future CLIC collider with particular emphasis on the physics requirements and the beam-induced background conditions including the resulting challenges in terms of track performance. It concludes with a brief description of the tracking system for CLICdet. In Section 3 the event simulation and software framework are presented. Section 4 presents the track reconstruction process at CLIC. The tracking performance in terms of efficiency, fake rate, track resolution and CPU time is shown in Section 5, while conclusions are presented in Section 6.

## 2 Tracking challenges at CLIC

CLIC is a proposed  $e^+e^-$  collider operating in three stages at centre-of-mass energies of 380 GeV, 1.5 TeV and 3 TeV, each stage lasting 7 – 8 years [1, 2, 3]. CLIC’s main goals are to measure the properties of the top quark and the Higgs boson with high precision and to search for physics beyond the Standard Model.

In order to reach its design luminosity of  $1.5 - 6 \times 10^{34} \text{ cm}^{-2} \text{ s}^{-1}$ , CLIC will operate with very small bunch sizes [1, 2, 4]. CLIC’s bunch sizes lead to strong beamstrahlung radiation from the electron and positron bunches in the field of the opposite beam. The interactions involving beamstrahlung photons result in two main types of background, incoherent  $e^+e^-$  pairs and  $\gamma\gamma \rightarrow$  hadron events. Both backgrounds are expected to affect the tracking performance in terms of detector occupancy. The incoherent  $e^+e^-$  pairs are mostly emitted in the forward direction and constrain the inner detector radius to  $\geq 31$  mm in the central region of the detector. The  $\gamma\gamma \rightarrow$  hadron events extend to larger angles with respect to the beam line, thus impacting the physics measurements. At the 3 TeV stage, each bunch train contains 312 bunches, separated by 0.5 ns. The bunch trains are separated by 20 ms.

An accurate vertex reconstruction is needed to obtain an accurate and efficient identification of secondary vertices from heavy-quark flavour hadrons and tau-leptons. This requirement translates to a transverse impact-parameter resolution at the level of  $\sigma_{d_0}^2 = (5 \mu\text{m})^2 + (15 \mu\text{m GeV})^2 / (p^2 \sin^3 \theta)$  and thus to a single point resolution of 3  $\mu\text{m}$  for the vertex detector, the innermost detector of CLICdet [4, 5]. The vertex detector is made of  $25 \times 25 \mu\text{m}^2$  pixels which are arranged in three cylindrical double-layers in the central region of CLICdet and in double-layer petals in a spiral arrangement in the forward direction allowing for efficient air cooling of the entire vertex detector.

In terms of track reconstruction, the scientific goals of CLIC place also a demanding requirement on the transverse momentum resolution for high-momentum tracks in the central detector region, which must be at the level of  $\sigma_{p_T}/p_T^2 \leq 2 \times 10^{-5} \text{ GeV}^{-1}$ . Optimization studies show that a tracker with a radius of 1.5 m immersed in a magnetic field of 4 T with a single point resolution smaller than 7  $\mu\text{m}$  will achieve the required resolution [4]. Therefore, a tracking detector made of silicon elongated pixel layers is placed around the vertex detector.

To fulfil the stringent requirements from the physics programme, the material budget of the CLICdet tracker must be limited to 0.2% radiation length ( $X_0$ ) per single layer in the vertex detector and  $1 - 2\% X_0$  per layer in the tracker. This ultra-light tracker with an extremely precise hit-position resolution is placed in the innermost part of CLICdet as shown in Figure 1(a). Its total amount of material expressed in term of radiation length  $X_0$  is shown in 1(b) and corresponds to about 4% nuclear interaction lengths in the central detector region.

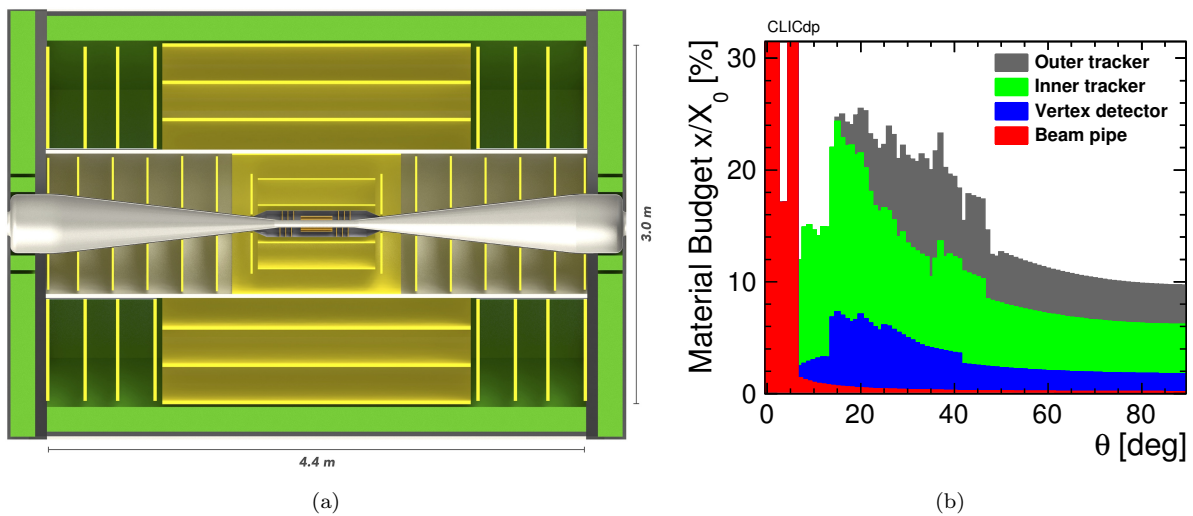


Figure 1: (a) Tracking system layout in CLICdet [4]. The vertex-detector layers are shown in orange, while the main tracker layers are depicted in yellow. The tracker is surrounded by the electromagnetic calorimeter, depicted in bright green. (b) The total thickness  $x$  of the tracker material as a function of the polar angle and averaged over azimuthal angles, expressed in units of radiation length  $X_0$  [6].

### 3 Event simulation and reconstruction

The performance of the track reconstruction algorithm used in CLICdet is estimated with full simulation studies. The full tracker geometry including the support material, cables and cooling is described with the DD4hep software [7] and simulated in GEANT4 [8] and includes a homogeneous solenoid field of 4 T.

To assess the tracking performance, two types of events are simulated and reconstructed. The first sample contains single muons and possible secondary particles produced by interaction with material. The second sample represents a more complex scenario where a jet topology event, an  $e^+e^- \rightarrow t\bar{t}$  event at 3 TeV centre-of-mass energy, is generated with WHIZARD [9] and the  $\gamma\gamma \rightarrow$  hadron background expected at the 3 TeV CLIC energy stage is superimposed [10]. The  $\gamma\gamma \rightarrow$  hadron background overlaid corresponds to a total of 30 bunch crossings (BX), 10 bunch crossings before and 20 bunch crossings after the physics event. The  $t\bar{t}$  event at 3 TeV produces on average about 90 tracks, which increases to about 550 tracks when the  $\gamma\gamma \rightarrow$  hadron background is overlaid.

The CLIC track reconstruction software is implemented in the linear collider Marlin framework [11] and interfaced with the geometry using DD4hep [12]. Large simulation and reconstruction samples were produced with the iLCDirac grid production system [13].

### 4 Track reconstruction

The main goal of the track reconstruction process is to estimate the momentum and position parameters of charged particles crossing the detector in a magnetic field. The first step of the track reconstruction is to create *reconstructed* hits. In CLICdet, the local position of the *simulated* hits from charged particles crossing the sensitive layers of the detector are smeared with a Gaussian distribution with a width equal to the single point resolution of the subdetector. This procedure is done for all simulated hits. The reconstructed hits are used as input for the subsequent steps of the track reconstruction.

The CLIC track reconstruction can be divided in three main blocks: the track finding with the conformal tracking algorithm, the track fitting using a Kalman filter and smoother, and the track selection. The final output of the track reconstruction are tracks which include not only the hits they are made of, but also the information of the estimated track parameters.

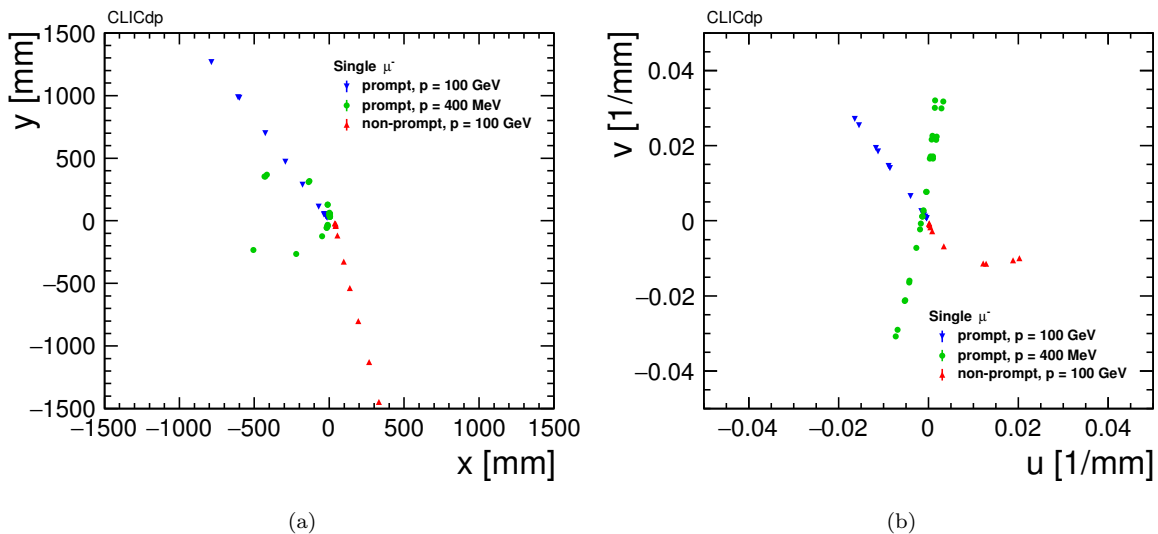


Figure 2: Hits produced by three muon tracks: prompt (blue), prompt with low momentum (green) and non-prompt (red). Tracks are shown in the  $(x, y)$  global coordinate system (a) and in the  $(u, v)$  conformal coordinate system (b).

#### 4.1 Track finding with the conformal tracking method

In the conformal algorithm, point coordinates in global space  $(x, y)$  are translated into the conformal space  $(u, v)$ . The idea behind this coordinate transformation is that circles passing through the origin of a cartesian coordinate system  $(x, y)$ , can be transformed into straight lines in a different coordinate system where the coordinates are defined as:

$$u = \frac{x}{x^2 + y^2}, \quad v = \frac{y}{x^2 + y^2}. \quad (1)$$

This is demonstrated in [14] and is valid if the circle is passing through the origin. In the conformal space  $(u, v)$ , the circle equation  $(x - a)^2 + (y - b)^2 = r^2$  is translated into a straight line

$$v = -\frac{a}{b}u + \frac{1}{2b}. \quad (2)$$

Through the application of the conformal algorithm, curved tracks left by charged particles bent by a magnetic field can be reduced to a straight lines search. The radial order of the hit positions is inverted in the conformal space with respect to the global space: track hits on the vertex detector layers correspond to larger  $(u, v)$  coordinates than hits on the tracker layers.

In real measurements not all particle trajectories can be approximated by a straight line due to possible deviations caused by particles undergoing multiple scattering or simply not originated at the origin of the  $(x, y)$  plane, also known as *displaced* or *non-prompt* particles. An example of each of these three cases is given in Figure 2 where hits belonging to three muon tracks are simulated using CLICdet. To take these deviations systematically into account, pattern recognition in conformal space is performed via a cellular automaton (CA) [15].

In the CA, cells are defined as segments connecting two hits and the algorithm is based on the creation and extension of these cells. The role of the CA in the conformal tracking is two-fold: firstly, it builds the so-called cellular track candidates and then, these cellular track candidates are extended to create full tracks and only those with the highest quality are selected.

#### 4.1.1 Building of cellular track candidates

The hit collection given as input to the building step is referred to as the *seeding collection* and each hit in the collection is considered as a *seed hit*, the starting point of a cellular track candidate. From each seed hit, one or more *seed cells* are created connecting the seed hit with its nearest neighbours. The nearest neighbour is defined as a hit which is within a certain angular region and distance from the seed hit, does not lie on the same detector layer, is located at a smaller conformal radius and is not already part of a track. Each seed cell is then extended to *virtual hits*, i.e. hits sitting on the prolongation in the radial direction of the cell, from which the search for nearest neighbours is repeated. New cells are then created and attached to the seed cell if the neighbouring hits do not lie on the same detector layer as the end point of the seed cell, have smaller conformal radius and had not been already included in a track. The extension of the new cell is then repeated and more cells are created. Each cell contains information about its start and end point as well as a *weight* information. The weight of a cell indicates how many other cells are further connected to it. Each subsequent link increments the cell weight by one unit, such that the higher the weight, the higher the potential of the cell to make a track.

Cellular track candidates are chains of cells, created by all cells compatible within a certain angle window starting from the highest weighted seed cell. A minimum number of hits for each candidate is required. Among all the cellular track candidates only those with the best quality are kept. This step is called *clone treatment* and it assesses the candidate quality using the length of the track and the two  $\chi^2$  independently computed using a linear regression fit on the conformal space and on the  $(s, z)$  plane, where  $s$  is the coordinate along the helix arc segment. Longer tracks are preferred, while the one with the best  $\chi^2$  is chosen in case of equal length. A further attempt to recover rejected cellular tracks is made by removing, one by one, each hit on the track, refitting and recomputing the normalised  $\chi^2$ . This allows one to keep good tracks that contain a spurious hit. At the end of the process, all hits belonging to the created cellular tracks are marked as *used*.

#### 4.1.2 Extension of cellular track candidates

The hit collection given as input of this CA step is used to extend the cellular track candidates created at the end of the building algorithm. Cellular track candidates are extended in different ways according to their particle transverse momentum estimated using the parameters extracted from the linear regression fit in the  $(s, z)$  space. All candidates with an estimated  $p_T$  above a threshold defined as external parameter are extended first, as they are easier to reconstruct.

In this case, the extension proceeds in a similar manner as described for the building step: end points of the previously formed cellular tracks are used as seed hits and a search for nearest neighbours in polar angle is performed. The search is performed limiting the compatible hits in the successive detector layers. New cellular tracks are created including every valid neighbour. Among those, the best track candidate is chosen based on the  $\chi^2$  values from the linear regression fit in  $(u, v)$  and  $(s, z)$ . If no hit is found on one layer, the cellular automaton proceeds on the subsequent layer. The extension process is repeated until the last detector layer.

The extension algorithm then is performed for cellular track candidates whose estimated  $p_T$  is lower than the threshold. To allow the reconstruction of very low- $p_T$  tracks, such as particles looping in the tracker, no specific nearest neighbour search is performed but all unused hits which are not located on the other side of the detector in  $z$  are considered for track extension. In this part, the search for compatible hits is done including a quadratic term in the regression formula, in order to take into account deviations from a straight line. At the end of the extension, all CA track candidates are sorted by  $p_T$  and the hits included in the conformal tracks are marked as *used*.

#### 4.1.3 Full conformal tracking chain

The two main CA algorithms are run on all reconstructed hits in several iterations with different sets of parameters. The full chain used in the CLIC track reconstruction is shown in Table 1. The first part aims to reconstruct the prompt tracks in the vertex detector: step 0 builds cellular track candidates using the hits in the vertex barrel as input, and they are extended in step 1 using the hits in the vertex endcap. The remaining hits in the combined vertex barrel and endcap detectors are then used to recover prompt tracks

Table 1: Overview of the configuration for the different steps of the pattern recognition chain. The last column shows some of the parameters of relevance for the cellular automaton as used for CLICdet: the maximum angle between cells, the maximum cell length, the minimum number of hits on a track, the maximum  $\chi^2$  for valid track candidates, and the  $p_T$  threshold used to discriminate between the two variations of the algorithm of track extension.

Step	Algorithm	Hit collection	Parameters				
			max cell angle [rad]	max cell length [mm <sup>-1</sup> ]	min $N_{\text{hits}}$	$\chi^2$ cut	$p_T$ threshold [GeV]
0	Building	Vertex Barrel	0.005	0.02	4	100	-
1	Extension	Vertex Endcap	0.005	0.02	4	100	10
2	Building	Vertex	0.025	0.02	4	100	-
3	Building	Vertex	0.05	0.02	4	2000	-
4	Extension	Tracker	0.05	0.02	4	2000	1
5	Building	Vertex & Tracker	0.05	0.015	5	1000	-

more difficult to find. This is done in two steps using tighter cuts first (step 2) and looser cuts afterwards (step 3). All cellular track candidates reconstructed in steps 2 and 3 are then extended to the hits belonging to the tracker detectors in step 4. The last part of the full chain focuses on the reconstruction of non-prompt particles (step 5) using the whole tracking system. During this step the CA is run from the outermost layer of the tracker back to the innermost layer of the vertex detector. Moreover, a quadratic term is included in the regression formula used to fit the cellular track candidates in conformal space. An example of all cellular track candidates reconstructed using the conformal tracking algorithm is given in Figure 3.

## 4.2 Track fitting and selection

The track fit in CLICdet consists of a Kalman filter and smoother in the global  $(x, y)$  coordinate space [16]. The fit is initialised with the parameters obtained by a simple helix fit to three hits of the track – typically first, middle, and last hit. The Kalman filter and smoother is then run as implemented in the Kallib package described in [17]. If the fit fails, the Kalman filter and smoothing procedure is tried again backwards.

In the track selection, some cuts are applied to the track candidates to filter out the tracks that contain many spurious hits or share a number of hits with other tracks. In order to do that, the clone treatment described in Section 4.1.1 is performed on the fitted track collection. The  $\chi^2$  used to determine the highest quality track is the one calculated at the end of the Kalman filter and smoother procedure. Moreover, only tracks with a number of hits larger or equal to three is kept to maximise the track efficiency.

## 5 Performance

In this section, the performance of the track reconstruction for the CLICdet experiment is investigated for simulated isolated muons and realistic topologies in a high occupancy environment.

The tracking efficiency is defined as the ratio of *pure* tracks to the number of reconstructable particles, i.e. simulated particles which are stable, and have  $p_T > 100$  MeV,  $|\cos(\theta)| < 0.99$ , and at least 4 hits on different layers. Pure tracks are defined as reconstructed tracks which have at least 75% of their hits associated to a single reconstructable particle. The efficiency is presented as a function of various parameters of the simulated particles.

The fake rate is defined as the ratio of *fake* tracks to the total number of reconstructed tracks. Fake tracks are defined as reconstructed tracks which have less than 75% of their hits associated to one reconstructable particle. The fake rate is presented as a function of various parameters of the reconstructed track.

The resolution for a specific track parameter is estimated from the track parameter residuals, defined as the difference between the reconstructed-track parameter and the simulated-particle parameter. The

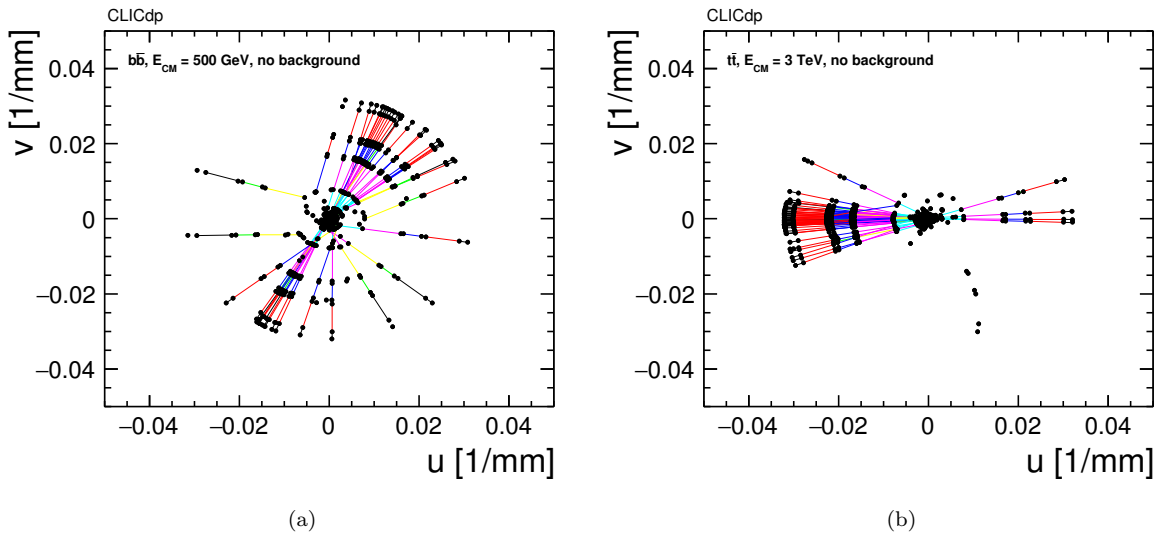


Figure 3: Cellular track candidates reconstructed for a single  $b\bar{b}$  event at 500 GeV centre-of-mass energy (a) and for a single  $t\bar{t}$  event at 3 TeV (b).

distribution of residuals is fitted with a Gaussian function, whose standard deviation defines the resolution.

## 5.1 Results for isolated muons

The tracking efficiency for single isolated muons is shown in Figure 4(a) as a function of the polar angle of the simulated particle. The tracking is fully efficient in the entire tracker acceptance and for any transverse momentum [6], while the fake rate is negligible.

The resolutions of the following track parameters were studied using simulated isolated muons [6]: transverse and longitudinal impact parameter, azimuthal and polar angle, and transverse momentum. High-momentum tracks fulfil the requirements on the impact parameter and transverse momentum set by the physics programme at CLIC as described in Section 2. As expected, all track parameter resolutions deteriorate in the forward region and for low-momentum tracks due to multiple scattering. Moreover, for high-momentum tracks resolutions of the impact parameters achieve the limit foreseen by the assumption on the single point resolution in the vertex detector. As an example, Figure 4(b) shows the resolution of the transverse momentum parameter as a function of the  $p_T$  of the simulated muon produced at  $\theta = 10^\circ$ ,  $30^\circ$ ,  $50^\circ$ ,  $70^\circ$  and  $89^\circ$ .

## 5.2 Results for complex events

The robustness of the track reconstruction at CLIC is estimated using more complex events in a realistic CLIC environment. Simulated  $e^+e^- \rightarrow t\bar{t}$  events at 3 TeV centre-of-mass energy with and without the  $\gamma\gamma \rightarrow$  hadron background expected at the 3 TeV energy stage of CLIC are used for this study.

In Figure 5 the efficiency and fake rate are shown as a function of the  $p_T$  of the simulated particle and of the reconstructed track, respectively. The tracking is fully efficient for simulated particles with  $p_T > 1$  GeV and the efficiency is still well above 90% down to a  $p_T$  approximately of 200 MeV. Both efficiency and fake rate are almost unaffected by the  $\gamma\gamma \rightarrow$  hadrons background expected at the 3 TeV energy stage of CLIC.

Results were also studied as a function of the smallest distance between the particle associated to the track and any other particle and as a function of particle production vertex radius. The efficiency plots are shown in Figure 6. The maximum efficiency loss for tracks produced in the vertex detector amounts to only 1% for  $\Delta_{MC} < 0.02$  rad. The tracking is fully efficient provided that the particles are produced within the

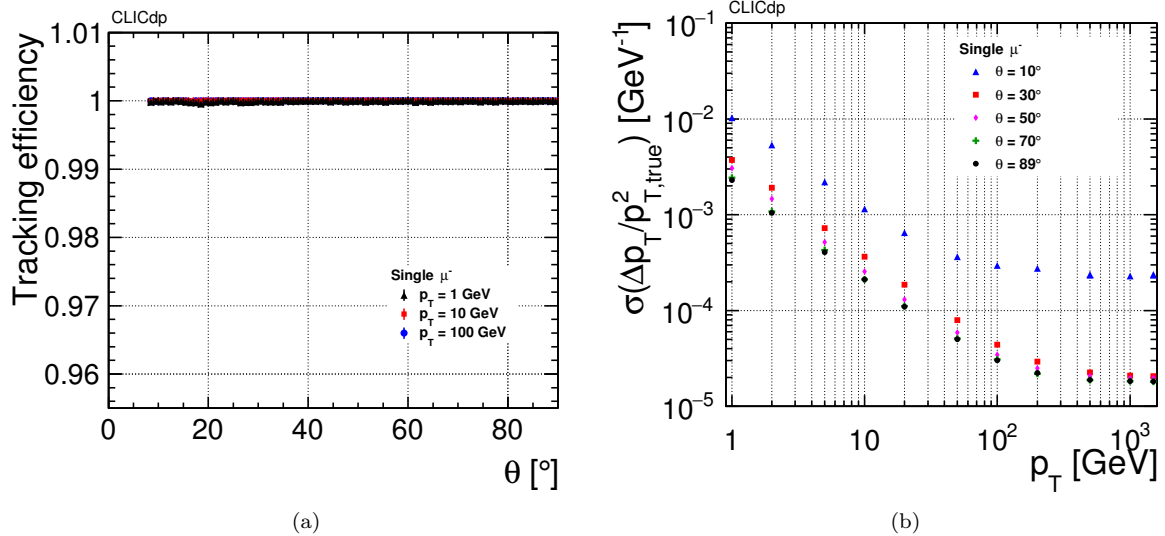


Figure 4: (a) Track reconstruction efficiency as a function of polar angle  $\theta$  for  $p_T = 1$  GeV, 10 GeV, and 100 GeV for isolated muons reconstructed with the CLICdet tracker. (b) Transverse momentum resolution for isolated muons with polar angle  $\theta = 10^\circ, 30^\circ, 50^\circ, 70^\circ$  and  $89^\circ$  as a function of  $p_T$ .

vertex detector.

Thanks to the conformal tracking modularity, the track reconstruction in CLIC was successfully adapted also to the CLD detector at FCC-ee which not only has a different sub-detector design and magnetic field magnitude but also includes different background conditions [18, 19].

### 5.3 CPU execution time

Like in many other particle physics experiments, track reconstruction is one of the most time consuming parts of the event reconstruction. A first assessment was performed using the mean CPU time of ten  $t\bar{t}$  events at 3 TeV centre-of-mass energy without and with the overlay of  $\gamma\gamma \rightarrow$  hadrons background expected at the 3 TeV energy stage of CLIC. If the background is not included, most of the CPU time is spent in the fitting procedure, otherwise the last CA building step (step 5) is the most time consuming part.

## 6 Conclusions

The conformal tracking presented in this paper is a new pattern recognition technique for track finding in the context of future electron–positron colliders. It uses a cellular automaton algorithm to find efficiently prompt and non-prompt tracks in conformal space and it has been demonstrated that it reconstructs tracks successfully also in the most challenging low- $p_T$  regime. Its robustness against the beam-induced backgrounds was proven using more complex events for the highest energy stage of CLIC. Moreover, some preliminary studies in terms of CPU computing time were also presented. Its use in the Particle Flow Analysis foreseen for particle reconstruction at future electron–positron colliders is essential [6] and will trigger further improvements in the near future.

## References

- [1] L. Linssen et al., "CLIC Conceptual Design Report: Physics and Detectors at CLIC," CERN-2012-003 (2012) [arXiv:1202.5940].



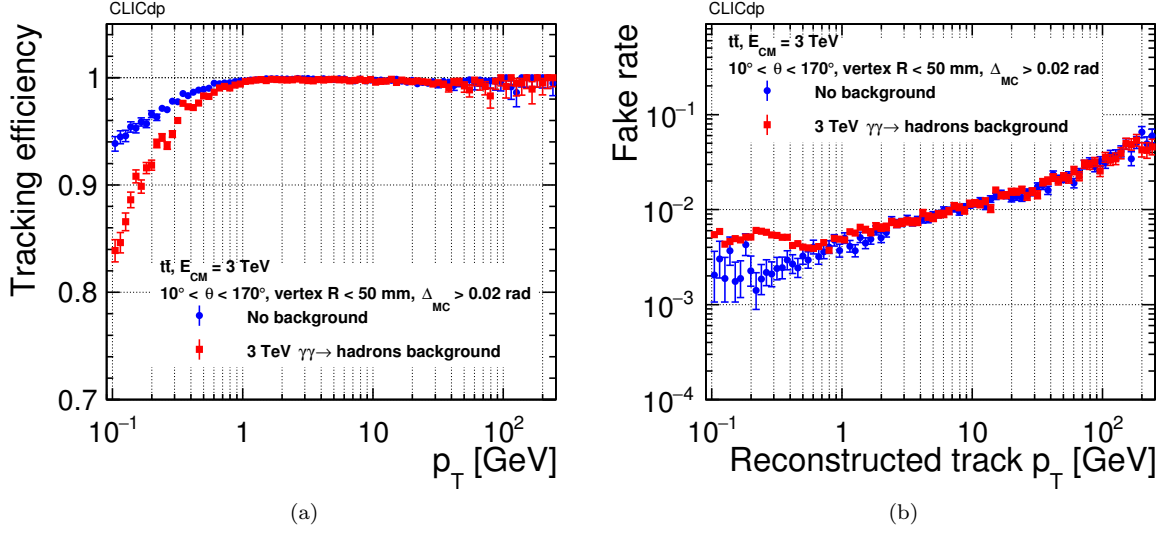


Figure 5: Tracking efficiency (a) and fake rate (b) as a function of the  $p_T$  of the simulated particle and of the reconstructed track, respectively.  $e^+e^- \rightarrow t\bar{t}$  events simulated at 3 TeV centre-of-mass energy are used with and without the corresponding overlay of 30 BX of  $\gamma\gamma \rightarrow$  hadrons background expected at the 3 TeV energy stage of CLIC.

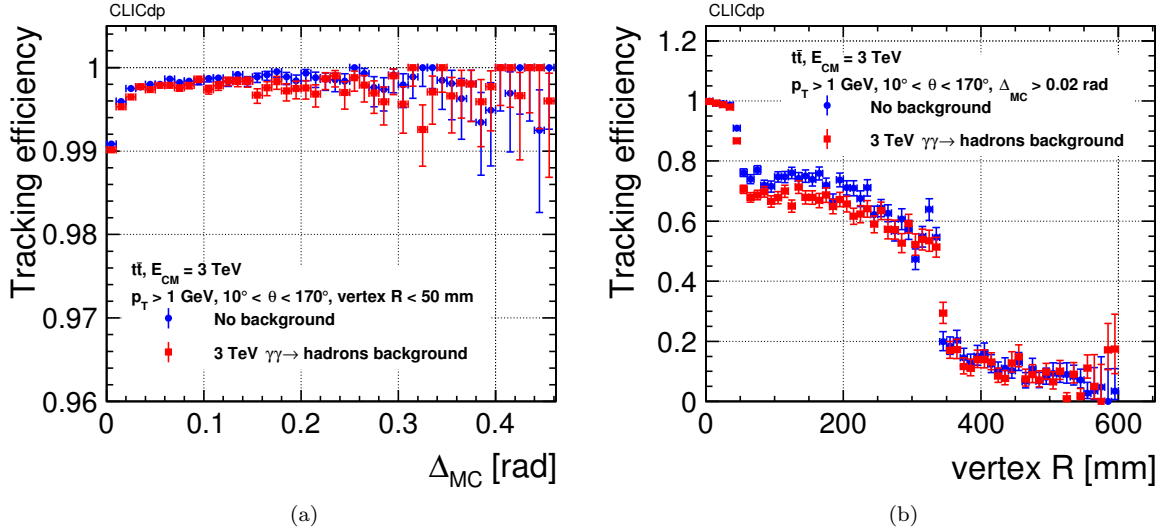


Figure 6: Tracking efficiency as a function of particle proximity (a) and of the particle production vertex radius (b).  $e^+e^- \rightarrow t\bar{t}$  events simulated at 3 TeV centre-of-mass energy are used with and without the corresponding overlay of 30 BX of  $\gamma\gamma \rightarrow$  hadrons background expected at the 3 TeV energy stage of CLIC.

- [2] P. Burrows et al., "Updated baseline for a staged Compact Linear Collider," CERN-2016-004 (2016) [doi:10.5170/CERN-2016-004].
- [3] T. Charles et al., "The Compact Linear  $e^+e^-$  Collider (CLIC) – 2018 Summary Report," CERN-2018-005-M (2018) [arXiv:1812.06018].

- [4] D. Dannheim et al., "Detector Technologies for CLIC," CERN-2019-001 (2019) [arXiv:1905.02520].
- [5] N. Alipour Tehrani et al., "CLICdet: The post-CDR CLIC detector model", CLICdp-Note-2017-001 (2017) [<http://cds.cern.ch/record/2254048>].
- [6] D. Arominski et al., "A detector for CLIC: main parameters and performance", CLICdp-Note-2018-005 (2018) [arXiv:1812.07337].
- [7] M. Frank et al., "DD4hep: A Detector Description Toolkit for High Energy Physics Experiments", J. Phys. Conf. Ser. 513 (2013) [doi:10.1088/1742-6596/513/2/022010].
- [8] S. Agostinelli et al., "Geant4 A Simulation Toolkit", Nucl. Instrum. Meth. A506 (2003), [doi:10.1016/S0168-9002(03)01368-8].
- [9] W. Kilian et al., "WHIZARD: Simulating Multi-Particle Processes at LHC and ILC", Eur. Phys. J. C71 (2011), [doi:10.1140/epjc/s10052-011-1742-y].
- [10] P. Schade and A. Lucaci-Timoce, "Description of the signal and background event mixing as implemented in the Marlin processor OverlayTiming", LCD-Note-2011-006 (2011), [<https://cds.cern.ch/record/1443537>].
- [11] F. Gaede, "Marlin and LCCD: Software tools for the ILC", Nucl. Instrum. Meth. A559 (2006), [doi:10.1016/j.nima.2005.11.138].
- [12] A. Sailer et al., "DD4Hep Based Event Reconstruction", J. Phys. Conf. Ser. 898 (2017), [doi:10.1088/1742-6596/898/4/042017].
- [13] C. Grefe et al., "ILCDIRAC, a DIRAC extension for the Linear Collider community", J. Phys. Conf. Ser. 513 (2013), [doi:10.1088/1742-6596/513/3/032077].
- [14] M. Hansroul et al, "Fast circle fit with the conformal mapping method", Nucl. Instrum. Meth. A270 (1988) [doi:10.1016/0168-9002(88)90722-X].
- [15] I. Kisel, "Event reconstruction in the CBM experiment", Nucl. Instrum. Meth. A556 (2006) [doi:10.1016/j.nima.2006.05.040].
- [16] R. Frühwirth, "Application of Kalman filtering to track and vertex fitting", Nucl. Instrum. Meth. A262 (1987), [doi:10.1016/0168-9002(87)90887-4].
- [17] K. Fujii, "Extended Kalman Filter", [<http://www-jlc.kek.jp/subg/offl/kaltest/doc/ReferenceManual.pdf>].
- [18] E. Leogrando, "Conformal tracking for the CLIC detector", CLICdp-Conf-2018-004 (2018), [<http://cds.cern.ch/record/2630512>].
- [19] M. Benedikt et al., "Future Circular Collider", CERN-ACC-2018-0057 (2018), [<https://cds.cern.ch/record/2651299>].